

OPEN

Expression response of chalcone synthase gene to inducing conditions and its effect on flavonoids accumulation in two medicinal species of *Anoectochilus*

Lin Yang^{1,2}, Jun Cheng Zhang², Jing Tao Qu¹, Gang He³, Hao Qiang Yu¹, Wan Chen Li^{1*} & Feng Ling Fu^{1*}

Anoectochilus roxburghii and *Anoectochilus formasanus* are the major species of genus *Anoectochilus* used in traditional Chinese medicine for their abundant content of flavonoids and some other medicinal constituents. In recent years, their wild resources are gradually exhausted due to over-collection and ecological deterioration. Artificial cultivation and tissue culture are employed to increase production. In this study, the open reading frame, promoter and genomic sequences of the chalcone synthase (CHS) gene were cloned from these two species according to their transcriptome information, and used for expression analysis in response to the induction of phenylalanine, ultraviolet light and NaCl, and its effect investigation on accumulation of flavonoids. The results showed that the expression of the CHS genes was upregulated in response to these inductions and resulted in increasing accumulation of total flavonoids. However, the increased flavonoids induced by phenylalanine and ultraviolet light were mainly allocated into the anthocyanidin branch of flavonoids biosynthesis. Not only did it improved the medicinal value, but might have inhibitory effect on plant growth because of the increased malondialdehyde accumulation. Under the induction of appropriate concentration of NaCl, the medicinal constituents of flavonoids were increased without inhibition to plant growth.

Anoectochilus roxburghii and *Anoectochilus formasanus*, native to Fujian and Taiwan provinces of China respectively, are the major species of genus *Anoectochilus* of family Orchidaceae, used as herbal drug and health food in traditional Chinese medicine¹. They are used to treat tumor, cardiovascular disease, fatty liver, hepatitis and other diseases because of their abundant medicinal constituents such as flavonoids and polysaccharides²⁻⁷. Due to over-harvesting and ecological deterioration, their wild populations have been gradually exhausted, and a lot of effort has been made for artificial cultivation and tissue culture for rapid propagation⁸⁻¹⁰. However, the accumulation of the medicinal constituents in the cultivated plants may be different from the wild plants. It becomes important to investigate the effect of cultivation or tissue culture conditions to the accumulation of the medicinal constituents, as well as its molecular mechanism¹⁰⁻¹⁴.

Flavonoids are a large category of aromatic secondary metabolites ubiquitous in plant and fungus. These compounds include six major subgroups that are found in higher plants: the chalcones, flavones, flavonols, flavandiol, anthocyanins, and condensed tannins (or proanthocyanidins); a seventh group, the auronins, is widespread, but not ubiquitous^{15,16}. Most of these constituents have antioxidant properties¹⁷. The flavonol subgroup, including rutin (rutinoside), quercetin and kaempferol, is the major medicinal constituents of *A. roxburghii* and *A. formasanus*^{1,18,19}. In plants, flavonoids are biosynthesized through phenylpropanoid pathway from initial substrate phenylalanine (Phe). Chalcone synthase (CHS) catalyzes the conversion of 4-coumaroyl-CoA and 3 units of

¹Maize Research Institute, Sichuan Agricultural University, Chengdu, Sichuan, 611130, PR China. ²Medical Plant Exploitation and Utilization Engineering Research Center, Fujian Province University, Sanming University, Sanming, 365004, People's Republic of China. ³Key Laboratory of Medicinal and Edible Plants Resources Development of Sichuan Education Department, Sichuan Industrial Institute of Antibiotics, Chengdu University, Chengdu, 610052, PR China. *email: aumdym@sicau.edu.cn; ffl@sicau.edu.cn

malonyl-CoA to chalcone, 4 units of coenzyme A (CoA-SH) and carbon dioxide (CO₂). This is the committed step branching to biosynthesis of flavonol, isoflavone and anthocyanidin (Fig. S1)^{16,20}. The *CHS* gene has been cloned and characterized from *Phalaenopsis hybrid*²¹, a relative species of another genus of family *Anoectochilus*, as well as many other plants^{22–27}. Its expression is responsive to induction of Phe^{28,29}, ultraviolet light (UV)^{11,30–33}, NaCl^{11,34,35} and some other biotic and abiotic conditions.

However, genomic information has not been available for any species of genus *Anoectochilus*, and even there are few reports about their chromosome ploidy³⁶. It is difficult for homologous cloning of genes from any species of this genus. In the present study, transcripts were assembled from RNA sequencing (RNA-seq) data, and used to clone the open reading frame (ORF) and the genomic sequences of the *CHS* gene from *A. roxburghii* and *A. formosanus*. After function evaluation by bioinformatics analysis, subcellular localization, enzyme activity assay and heterologous expression, their expression response to induction of Phe, UV, and NaCl was measured by real-time quantitative PCR (RT-qPCR). Their promoter sequences were amplified by thermal asymmetric interlaced PCR (TAIL-PCR) and used for prediction of *cis*-acting elements. The contents of total flavonoids, free radical scavenging activity (FRSA), content of anthocyanidin and flavonols (rutin, quercetin, and kaempferol), as well as malondialdehyde (MDA), were measured by spectrophotometry and high performance liquid chromatography (HPLC), respectively. The possibility was explored to upregulate the expression of the *CHS* gene and to increase the accumulation of total flavonoids or flavonols in *A. roxburghii* and *A. formosanus* by induction in artificial cultivation or tissue culture.

Results

The *CHS* genes and their putative proteins. 8.76 and 10.42 Gb raw bases, and 29213781 and 34742855 raw reads were obtained by RNA-seq of the *A. roxburghii* and *A. formosanus* samples. Through quality inspection and filtration, 8.28 and 9.85 Gb clean bases, and 27597990 and 32836885 clean reads were retained, respectively, with Q20 (sequence error rate below 1%) greater than 96% and Q30 (sequence error rate below 0.1%) greater than 90% (Fig. S2). From these clean reads, 130024 and 116423 transcripts were assembled, 30265 and 24425 of them were annotated by SWISSPROT, and 35176 and 28691 of them were annotated by KGO, respectively. One of them was annotated as the *CHS* gene for *A. roxburghii* and *A. formosanus*, respectively. These two transcripts shared 94.80% similarity (Fig. S3).

With the primers homologous to the assembled transcripts, specific fragments of more than 1000 bp were amplified from the cDNA and the genomic DNA samples of *A. roxburghii* and *A. formosanus*, respectively (Fig. S4). The sequence analysis showed that their genomic fragments were both 1260 bp long and shared similarity of 94.92%. Their ORFs (1173 bp) were interrupted by an intron of 87 bp from the 180th to the 267th bp (Fig. S5). Their putative proteins (390 aa) were highly homologous (90.75% and 90.00%) with that of the *CHS* gene (AAV70116.1) in *P. hybrida* of family *Anoectochilus* (Fig. 1A)²¹. The predicted molecular weight (42.9 kDa), isoelectric points (pI 6.04 and 6.24), grand averages of hydropathicity (−0.116 and −0.123), secondary structure (31.54% and 32.82% α -helices, 21.54% and 20.51% extended strands, 46.92% and 46.67% random coils, respectively), and three three-dimensional structure models were all similar to that (42.5 kDa, pI 6.04 and −0.057, 29.74% α -helices, 21.03% extended strands, and 49.23% random coils) of the putative *CHS* protein in *P. hybrida* (Fig. S6)²¹. In the phylogenetic tree, the putative proteins of these two ORFs were also clustered into the same group with the putative *CHS* protein in *Phalaenopsis hybrida* (Fig. 1B). All the thirteen activation sites (G¹³⁸, G¹⁶³, G¹⁶⁷, L²¹⁴, D²¹⁷, G²⁵³, P³⁰⁵, G³⁰⁶, G³⁰⁷, G³³⁶, and G³⁸⁵, P³⁸⁶, G³⁸⁷), the four catalytic residues (Cys¹⁶⁴, Phe²¹⁵, His³⁰⁴ and Asp³³⁷) and the conserved domain of six residues (G³⁷⁹, V³⁸⁰, L³⁸¹, F³⁸², G³⁸³, F³⁸⁴) were the same, except the three amino acids different in the malonyl-CoA binding motif (V³¹⁴, E³¹⁵, E³¹⁶, R³¹⁷, V³¹⁸, G³¹⁹, L³²⁰, K³²¹, P³²², E³²³, K³²⁴, L³²⁵, T³²⁶, T³²⁷, S³²⁸, R³³⁰)²¹.

Function evaluation of the *CHS* genes. The green fluorescence signal was observed in the nucleus of the inner epidermis cell of onion transiently expressing vectors pCAMBIA2300-35S-*CHS*-eGFP, whereas it distributed in the whole cell infiltrated by the negative control vector pCAMBIA2300-35S-eGFP (Fig. 2). This result indicated the subcellular localization of the *CHS* protein in nucleus in *A. roxburghii* and *A. formosanus*.

By sodium dodecyl sulfate-polyacrylamide gel electrophoresis (SDS-PAGE), an obvious additional band about 44.3 kDa was separated from the *Escherichia coli* lines transformed by the *CHS* genes of these two medicinal species, and induced by isopropyl β -D-thiogalactopyranoside (IPTG) (Fig. S7). The *in vivo* *CHS* enzyme activities of the transformed *E. coli* lines of the *A. roxburghii* *CHS* gene was significantly higher than that transformed by the *A. formosanus* *CHS* gene, while the *in vitro* activities showed no significant difference (Figs. 3A,B and S8).

From the rice calli transformed by the *CHS* genes, three T₁ lines (two of *A. roxburghii* and one of *A. formosanus*) were identified as positive by PCR amplification of the *CHS* gene fragment (Fig. S9). Their contents of total flavonoids were 1.40, 1.68 and 1.26 times higher than that of the untransformed acceptor line, respectively (Fig. 3C).

All these results confirmed that the two amplified ORF sequences were the *CHS* genes of *A. roxburghii* and *A. formosanus*, respectively, and registered at GenBank with accession numbers MK370742 and MK370743.

Differential expression in response to inducing conditions. Under the induction of Phe and UV, the expression of the *CHS* genes was upregulated significantly in *A. roxburghii* and *A. formosanus*, and reached its peak values (81.53 and 7.49 times of the 0 h control, respectively) at 4 and 8 h of the Phe induction, and (21994.7 and 3654.7 times of the 0 h control, respectively) at 8 and 12 h of the UV induction (Fig. 4A,B). In response to the NaCl induction, the expression of the *CHS* genes was continually upregulated and reached about three times of the 0 h control in *A. roxburghii*, while the upregulated expression reached 36.2 and 19.5 times of the 0 h control at 2 and 12 h of the NaCl induction in *A. formosanus* (Fig. 4C). This result indicated the strong expression response of these two *CHS* genes.

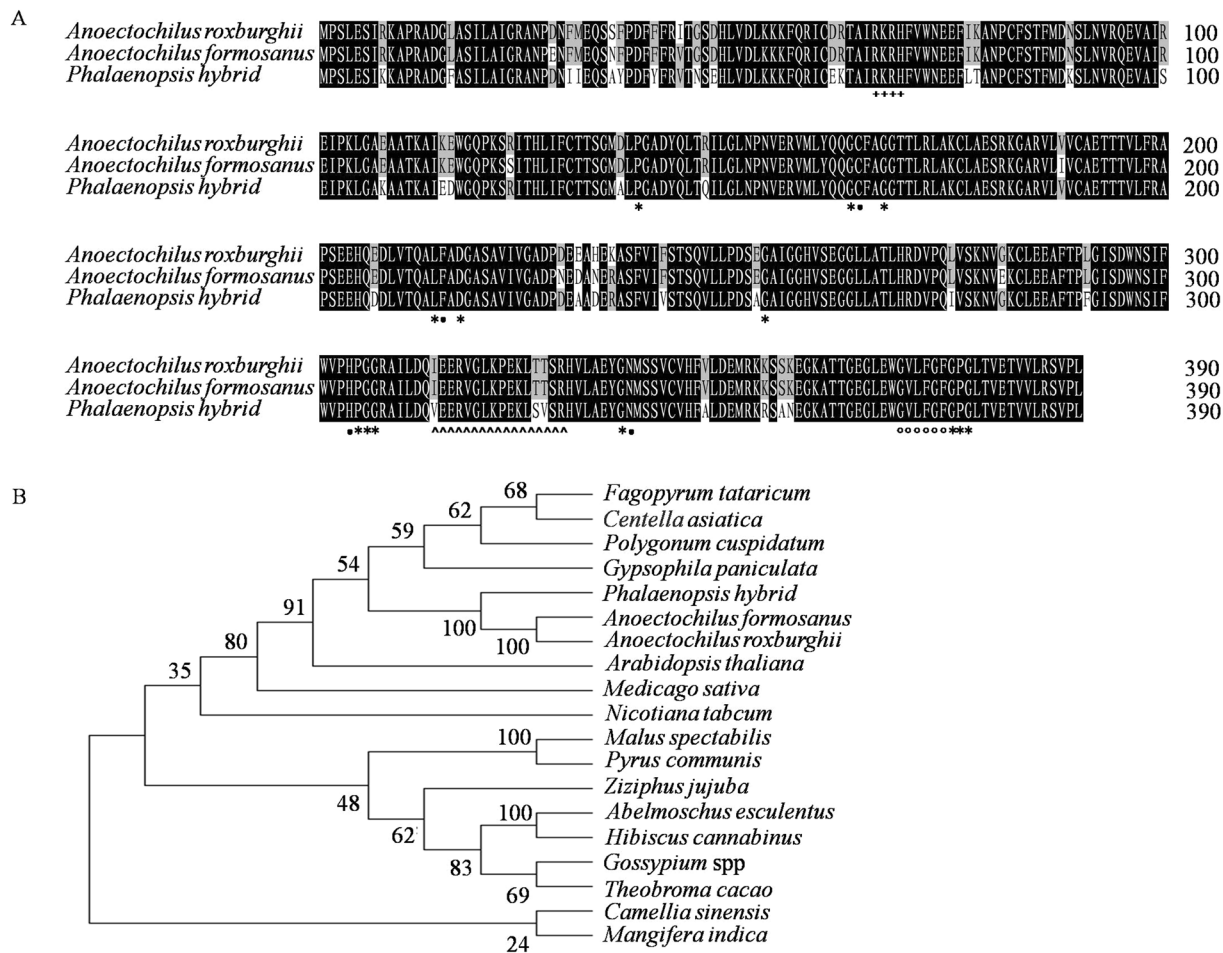


Figure 1. Alignment and phylogenetic tree of putative proteins of gene *CHS* of *A. roxburghii* and *A. formosanus* with relative species. (A) Alignment among the putative proteins of gene *CHS* of *A. roxburghii*, *A. formosanus* and *P. hybrida*. The black, gray and white backgrounds represent similarity of 100%, 66.7% and 0%, respectively. The asterisks (*), the black dots (●), the hollow dots (○), the hollow triangles (△) and the plus (+) represent the activation sites, the catalytic residues, the conserved residues, the malonyl-coenzyme A binding motif and the nuclear localization signal, respectively. (B) Phylogenetic tree among the putative proteins of gene *CHS* of 19 relative species.

From the products of the second and the third rounds of thermal asymmetric interlaced PCR (TAIL-PCR) amplification from the genomic DNA samples, specific fragments were separated and sequenced for prediction of promoters and *cis*-acting elements of the *CHS* genes by Plant CARE software (Fig. S10). The promoter sequence of the *CHS* gene of *A. roxburghii* was 342 bp long containing enhance elements TATA-box (4), 5'-UTR Py-rich stretch (1) and CAAT-motif (6), light responsive elements G-box (2), *sp1* (18) and I-box (1), and anaerobic inducing element ARE (1). The promoter sequence of the *CHS* gene of *A. formosanus* was 314 bp long containing enhance elements TATA-box (1), AT-rich sequence (1) and CAAT-box (5), light responsive elements G-box (2), CATT-motif (1), CGT-motif (5), GA-motif (1) and *sp1* (2), MeJA-responsive elements CGTCA-motif (1) and TGACG-motif (1), and anaerobic inducing element ARE (1) (Fig. S11). This result might partially explain the expression response of the *CHS* genes to the UV and NaCl induction.

Flavonoids accumulation under inducing conditions. Under non-inducing conditions (the 0 h control), the accumulation of total flavonoids, FRSA, and the accumulation of three flavonols (rutin, quercetin, and kaempferol) of *A. roxburghii* was 1.73, 1.52, 25.76, 5.48 and 6.02 times of that of *A. formosanus*, respectively (Fig. 5), indicating its higher antioxidant activity and medicinal value.

In response to Phe induction, the accumulation of total flavonoids and FRSA in *A. roxburghii* and *A. formosanus* was both increased and reached their peak values (1.38, 1.51, 1.30, and 2.06 times of the 0 d control) on the 5th, 3rd, and 4th day, respectively (Fig. 6A,B). The difference of total flavonoids content was not significant between these two species, but the increased range of FRSA in *A. roxburghii* was significantly lower than that in *A. formosanus*. The accumulation of rutin, quercetin and kaempferol was decreased during the first three days of the induction but rebounded after that with different ranges between the two species (Fig. 6C–E). The accumulation of anthocyanidin and MDA was increased continually with different ranges between the two species (Fig. 6F,G).

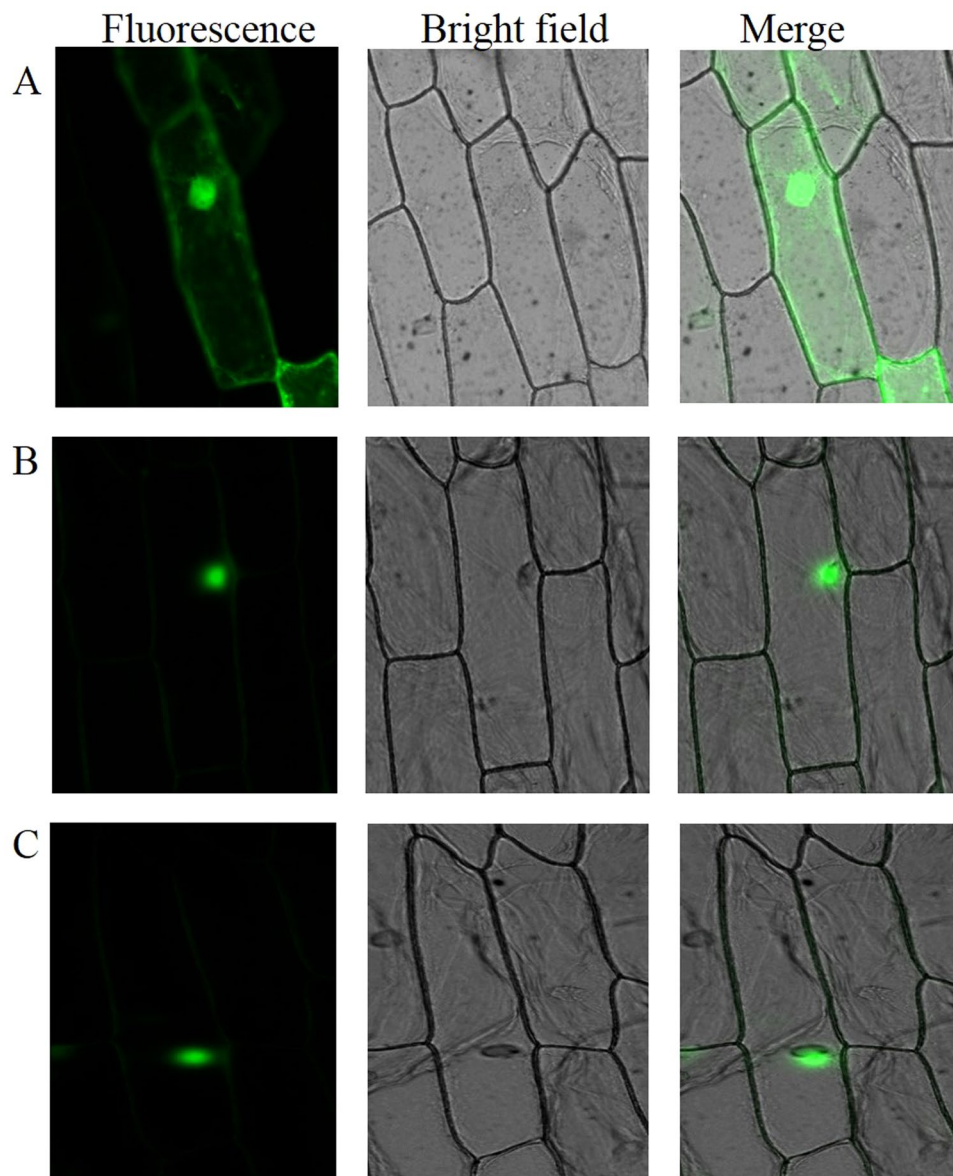


Figure 2. Subcellular localization of CHS protein. (A) Negative control transformed by empty vector pC2300-35S-*eGFP*. (B) Transient expression of vector pC2300-35S-*CHS-eGFP* harboring the *A. formosanus* *CHS* gene. (C) Transient expression of vector pC2300-35S-*CHS-eGFP* harboring the *A. roxburghii* *CHS* gene.

Under UV induction, the accumulation of total flavonoids and FRSA in the two species was increased and reached their peak values (2.09, 2.01, 1.47, and 1.82 times of the 0 h control) on the 5th, 4th, 3rd, and 2nd day, respectively (Fig. 7A,B). The accumulation of rutin, quercetin and kaempferol was decreased and rapidly descend to their valley values on the 1st to 5th day (Fig. 7C–E). The accumulation of anthocyanidin and MAD was increased continually (Fig. 7F,G).

In response to NaCl induction, the accumulation of total flavonoids and FRSA was increased continually with different ranges between *A. roxburghii* and *A. formosanus* (Fig. 8A,B). The rutin accumulation in *A. roxburghii* was increased sharply on the 5th and 6th day and reached as high as 21.28 times of the 0 h control, whereas that in *A. formosanus* did not changed obviously (Fig. 8C). The accumulation of quercetin, kaempferol and anthocyanidin was increased with different ranges between the two species (Fig. 8D–F). The MAD content was only increased slightly (1.23 and 1.26 times of the 0 h control, Fig. 8G).

Discussion

Numerous studies showed that the biosynthesis of flavonoids, as well as flavonols, took place exclusively in endoplasmic reticulum, cytosol, and other cytoplasmic organelles^{19,36–38}. In this study, the subcellular localization of the CHS proteins of *A. roxburghii* and *A. formosanus* was targeted to the nucleus (Fig. 2). This result was also evidenced by the bioinformatics prediction of a nuclear localization signal (Arg⁶⁶-Lys⁶⁷-Arg⁶⁸-His⁶⁹) at the N-terminal of their primary structure (Fig. 1A). Some recent reports from a number of different plant species

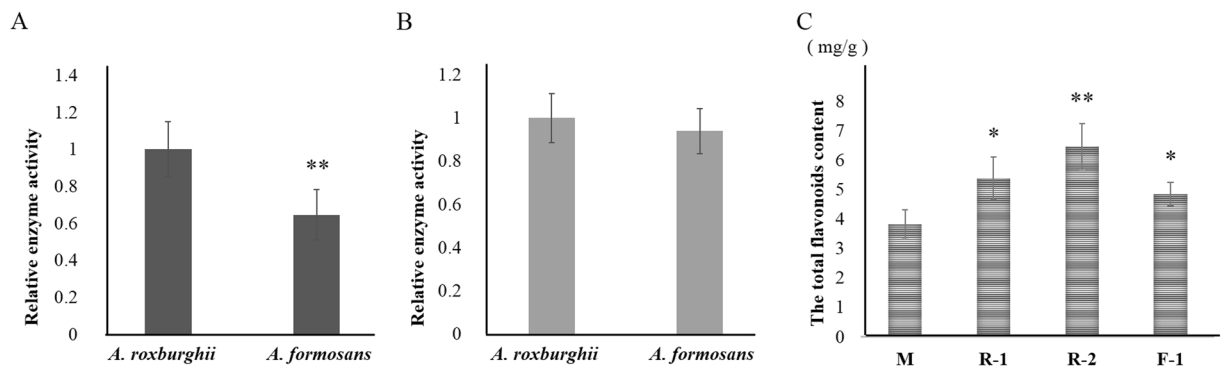


Figure 3. Relative enzyme activity of *E. coli* strains and total flavonoids content of rice lines heterologously-expressed CHS protein of *A. formosanus* and *A. roxburghii*. The asterisk (*) and the double asterisk (**) stand for significance ($P \leq 0.05$) and great significance ($P \leq 0.01$), respectively. (A) *in vitro* enzyme activity. (B) *in vivo* enzyme activity. (C) The total flavonoids content in transgenic rice lines F-1 (transformed by the *A. formosanus* CHS gene), R-1 and R-2 (transformed by the *A. roxburghii* CHS gene).

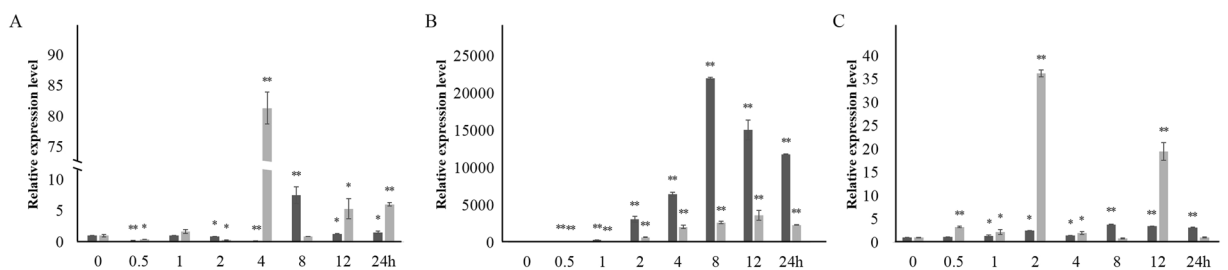


Figure 4. Relative expression levels of gene CHS of *A. roxburghii* and *A. formosanus* under Phe, UV and NaCl induction. The lighter and the darker columns represent *A. roxburghii* and *A. formosanus*, respectively. The asterisk (*) and the double asterisk (**) stand for significance ($P \leq 0.05$) and great significance ($P \leq 0.01$), respectively. (A) Phe induction. (B) UV induction. (C) NaCl induction.

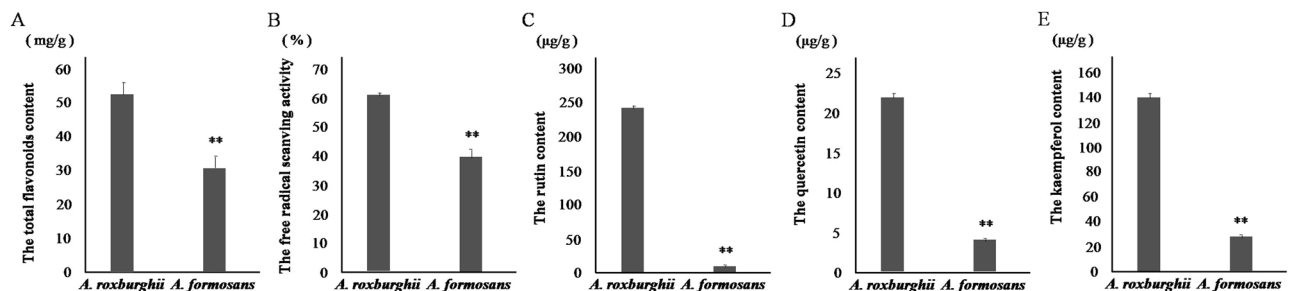


Figure 5. Content of total flavonoids and flavonols, and FRSA in *A. roxburghii* and *A. formosanus* under non-inducing condition. The asterisk (*) and double asterisk (**) stand for significance with the control at 0.05 and 0.01 levels, respectively. (A) Content of total flavonoids. (B) FRSA. (C) Content of flavonols (rutin, quercetin and kaempferol).

not only documented the presence of flavonoids in nuclei^{39,40}, but also localized at least two of their biosynthetic enzymes to nuclei in several cell types in *Arabidopsis*⁴¹. It was speculated that the *Anoectochilus* CHS proteins might catalyze flavonoids synthesis of the phenylpropane metabolism pathway in nucleus, and their products might be involved not only in the basal metabolism, stress response, reproductive development and many other growth and development processes^{30–35}, but also in the transcriptional regulation of related genes.

Under Phe, UV and NaCl induction, the expression of the CHS genes of *A. roxburghii* and *A. formosanus* were upregulated with different ranges (Fig. 4). The *cis*-acting elements related to light and anaerobic response were predicted in the promoter sequences of the two CHS genes (Fig. S11)^{42–44}. These results not only explain the increased accumulation of total flavonoids in the two species under these inducing conditions, but also confirm the rate-limiting role of the CHS enzyme for flavonoids biosynthesis of phenylpropanoid pathway (Fig. S1)^{16,20–27}.

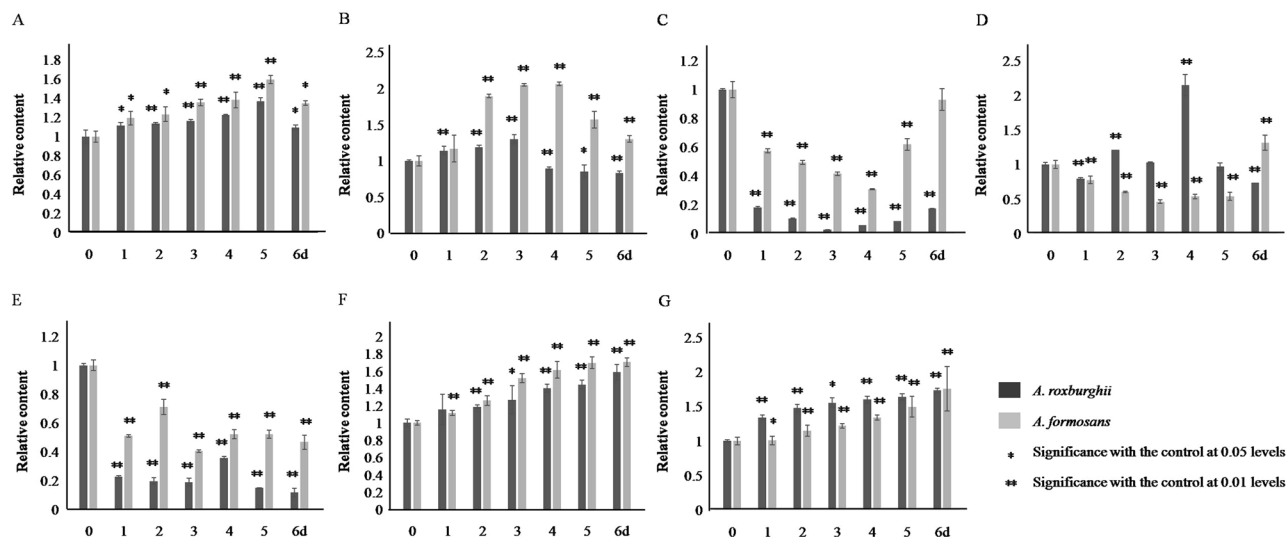


Figure 6. Content of total flavonoids, flavonols, anthocyanidin, and MDA, and FRSA in *A. roxburghii* and *A. formosanus* under Phe induction. The asterisk (*) and double asterisk (**) stand for significance with the control at 0.05 and 0.01 levels, respectively. (A) flavonoids content. (B) Free radical scavenging rate. (C) rutin content. (D) quercetin content. (E) kaempferol content. (F) Anthocyanidin content. (G) MDA content.

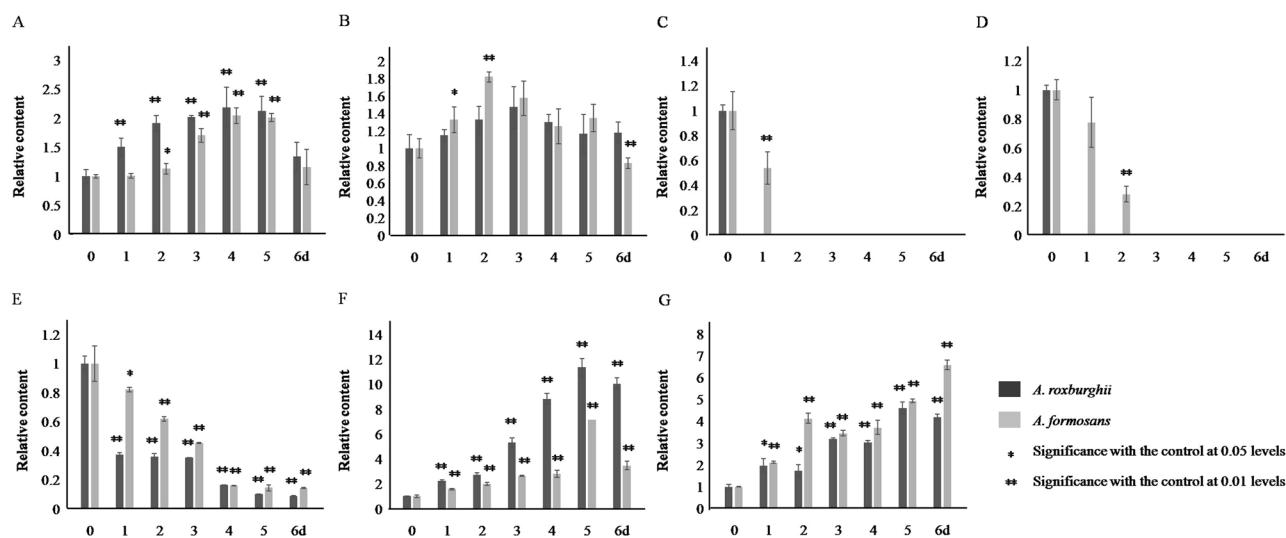


Figure 7. Content of total flavonoids, flavonol, anthocyanidin, and MDA, and FRSA in *A. roxburghii* and *A. formosanus* under UV induction. The asterisk (*) and double asterisk (**) stand for significance with the control at 0.05 and 0.01 levels, respectively. (A) flavonoids content. (B) Free radical scavenging rate. (C) rutin content. (D) quercetin content. (E) kaempferol content. (F) Anthocyanidin content. (G) MDA content.

Under Phe and UV induction, the decreased flavonols (Figs. 6C–E and 7C–E) and the increased accumulation of anthocyanidin (Figs. 6F and 7F) demonstrated that the increased accumulation of total flavonoids (Figs. 6A and 7A) was mainly allocated into the anthocyanidin branch of the phenylpropanoid pathway (Fig. S1). This was not conducive to improving medicinal value of these two species. Even more, the increased MDA accumulation revealed the inhibitory effect of Phe and UV on plant growth (Figs. 6G and 7G). Similar effect was also found in cell suspension culture of strawberry and calli of *Hydrocotyle bonariensis*^{28,29}. In response to NaCl induction, the increased flavonols (Fig. 8C–E), especially the sharp peak content of rutin on the 5th and 6th day of induction in *A. roxburghii*, indicated that the increased accumulation of total flavonoids (Fig. 8A) was mostly allocated into the flavonol branch (Fig. S1), while the MDA content was only increased slightly (Fig. 8G). Along with the higher accumulation of total flavonoids, FRSA, and the accumulation of flavonols in *A. roxburghii* under non-inducing conditions (Fig. 5), it was suggested that NaCl induction of appropriate concentration (100 mmol/L) in artificial cultivation or tissue culture of *A. roxburghii* could efficiently increase the accumulation of total flavonoids and flavonols, and improved the medicinal value.

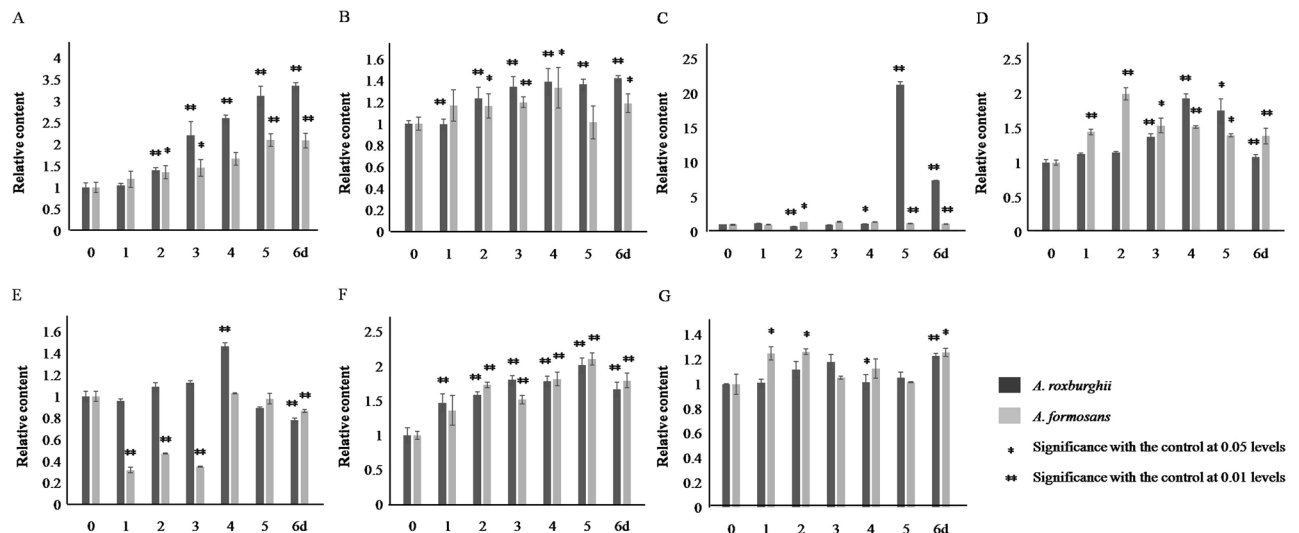


Figure 8. Content of total flavonoids, flavonols, anthocyanidin, and MDA, and FRSA in *A. roxburghii* and *A. formosanus* under NaCl induction. The asterisk (*) and double asterisk (**) stand for significance with the control at 0.05 and 0.01 levels, respectively. (A) flavonoids content. (B) Free radical scavenging rate. (C) rutin content. (D) quercetin content. (E) kaempferol content. (F) anthocyanidin content. (G) MDA content.

Conclusion

The Phe, UV and NaCl induction upregulates the expression of the chalcone synthase genes and affects the accumulation of total flavonoids, FRSA, flavonols, anthocyanidin and MAD in *A. roxburghii* and *A. formosanus*. NaCl induction of appreciate concentration (100 mmol/L) is suggested to apply in artificial cultivation or tissue culture of *A. roxburghii* to increase accumulation of total flavonoids and flavonols and improve the medicinal value.

Materials and Methods

Sample preparation. The seedlings of *A. roxburghii* and *A. formosanus* were cultured on MS medium for 18 weeks. The uniform seedlings were divided into three groups. Two groups were transplanted into a plastic mesh grid for aquaculture. On the fifth day, Phe and NaCl were added into the nutrient solution with final concentration of 4 mg/L and 100 mmol/L, respectively. The other group was transplanted into plastic pots (five seedlings per pot) with nutritional soil and vermiculite (3:1), and submitted to UV induction of 253.7 nm after recovering. At 0 (control), 0.5 h, 1 h, 2 h, 4 h, 8 h, 12 h, 24 h (1 d), 2 d, 3 d, 4 d, 5 d and 6 d of the Phe, UV and NaCl induction, two leaves were sampled from each of the five induced plants.

One leaf of each sample of 0 to 24 h of the induction was pulverized to fine powder in liquid nitrogen, and used for RNA extraction with RNeasy Plant Mini Kit (Qiagen, China). After release of probable DNA contamination by RNase-free DNase I (Qiagen, China), detection for concentration, purity and integrity on spectrophotometer (NanoDrop One, Thermo Fisher Scientific, USA) and Agilent 2100 Bioanalyzer (Agilent Technologies, USA) respectively, part of each RNA samples was reverse transcribed to cDNA by using PrimeScript RT Reagent Kit (TaKaRa Japan). Part of pulverized leaf samples of the control (0h) were mixed and used for extraction of genomic DNA with the method of cetyl trimethylammonium bromide (CTAB).

Transcriptome sequencing and CHS gene cloning. Part of the RNA samples of the control (0h) were mixed and sequenced by Illumina HiseqXten platform at MajorbioBioTech Co., Ltd. The clean reads were assembled by Trinity v2.4.0 (<https://github.com/trinityrnaseq/trinityrnaseq/wiki>), and used to search for transcript sequences of the *CHS* genes by SWISSPROT (<https://swissmodel.expasy.org/>) and KOG (<https://genome.jgi.doe.gov/Tutorial/tutorial/kog.html>). According to the transcript sequences, a pair of specific primers (Table S1) was synthesized and used to amplify the ORF and genomic sequences of the *CHS* genes from the cDNA and the genomic DNA samples, respectively, by using Prime STAR HS DNA Polymerase (TaKaRa, China) with proof reading activity. The amplified products were purified by using Universal DNA Purification Kit (Tiangen, China), added dATP at the 3' ends by using *Taq*TM (TaKaRa, China), cloned into pMD19-T vector (TaKaRa, Japan), and sequenced at Sangon Biotech Co., Ltd (Shanghai, China). The sequencing results were aligned for gene structure on NCBI website (<http://www.ncbi.nlm.nih.gov>), and predicted for putative proteins by using online tool SWISS-MODEL (<https://swissmodel.expasy.org/>). Phylogenetic analysis was conducted among the putative proteins by using MEGA7.0 software (<https://www.megasoftware.net/>).

Function evaluation of the CHS genes. Three pairs of specific primers with appropriate recognition sites (Table S1) were used to amplify the ORF sequences without or with the termination codons from the harbored pMD19-T vectors by using Prime STAR HS DNA Polymerase (TaKaRa, Japan). The amplified products were purified as above, and inserted into transient expression vector pCambia2300, prokaryotic expression vector pET-28a (+) and monocotyledonous expression vector pZZ00026, respectively, by using CloneExpress One Step Cloning Kit (Vazyme, China, Fig. S13).

The transient expression vectors pCAMBIA2300-35S-*CHS-eGFP* harboring the *CHS* genes of the two species, as well as the empty plasmid pCAMBIA2300-35S-*eGFP* (negative control), was infiltrated into the inner epidermis of onion. After incubation at 28 °C under dark for 24 h, the green fluorescence signal for subcellular localization was observed and photographed under fluorescence microscope (Olympus BX63, Japan)⁴⁵.

The prokaryotic expression vectors pET-28a (+)–*CHS* were transformed into *E. coli* train BL21 with freeze-thaw method. Until OD₆₀₀ ≈ 0.6, the transformant cultures were added with IPTG to a final concentration of 0.5 mmol L⁻¹, and incubated at 37 °C for 2 h. The heterologous expression of the *CHS* genes was detected by SDS-PAGE. The proteins were purified by using Ni-NTA Sefinose™ Resin Kit (Sangon China), and determined for concentration by using NanoDrop™ One/OneC B-50Q (Thermo, USA). According to the manual (Table S2) of CHS enzyme activity kit (Genmed Scientifics Inc. USA), the purified protein and the IPTG-induced *E. coli* cells were reacted with 4-coumaric-CoA and 3 units malonyl-CoA in the presence or absence of luteolin (a sensitive inhibitor of CHS), respectively. Along with the synthesis of chalcone, the released 4 units of CoA-SH with Ellman reagent 5,5-dithiobis (2-nitrobenzoic acid, DTNB) to produced yellow 5-thio-2-nitrobenzoic acid (TNB). The activity of chalcone synthase was quantitatively analyzed by the change of its absorption peak (412 nm wavelength). The *in vitro* and *in vivo* CHS enzyme activities were analyzed by the change of the absorption peak at 412 nm.

The monocotyledonous expression vector pZZ00026-*Ubi-CHS-T-nos* was mobilized into *Agrobacterium tumefaciens* strain EHA105, and used to transform rice calli of variety ZH11⁴⁶. The transformed lines were identified by PCR amplification of a 1205 bp fragment of the *CHS* genes, and detected for content of total flavonoids by spectrophotography (described later).

Expression analysis under inducing conditions. Two pairs of RT-qPCR primers (Table S1) was synthesized to amplify a 136 bp and a 221 bp fragment of the *CHS* ORF and the *Actin2* gene (used as internal reference), respectively, from the cDNA samples of the three replicates of each time point of the inducing treatments⁴⁷. The amplification reaction was conducted by using SsoFastEvaGreenSupermix (Bio-Rad, USA) in Bio-Rad iCycler iQ5 RT-qPCR System. The 2^{-ΔΔCT} method of the CFX Manger™ software version 2.0 (Bio-Rad, USA) was used to normalize the expression differentiation between the internal reference and the *CHS* gene⁴⁸. The relation expression levels under the inducing conditions were calculated by their expression level to those under the non-inducing control.

As described by Liu *et al.*⁴⁹, six arbitrary degenerate primers (AD) and three nested primers (Table S1) complementary to the coding sequences of the *CHS* genes were synthesized, and used to amplify the promoter sequences of the *CHS* genes from the genomic DNA samples by TAIL-PCR. The products of the second and third rounds of amplification were separated by 1.2% agarose gel electrophoresis, purified and sequenced as above. The sequenced results were used for prediction of *cis*-affecting elements by Plant CARE software (<http://bioinformatics.psb.ugent.be/webtools/plantcare/html/>).

Quantification of total flavonoids and free radical scavenging activity. The other leaf of each sample of 0 to 6 d of the induction was dried at 55 °C, ground to fine powder (extraction quality), extracted in 95% alcohol in an ultrasonic instrument at 25 °C for 30 min. The extracts were filtered through Whatman No. 1 paper filter under reduced pressure (extraction volume). Referring to China national standardization for determination of total flavonoids in propolis⁵⁰, 1 mL of each of the filtrates was added with 0.4 ml of 5% NaNO₂, kept for 5 min, added with 0.4 ml of 10% Al(NO₃)₃, kept for 5 min, added with 4 ml of 4% NaOH for coloration, incubated at room temperature for 20 min, and determined for absorbency at 420 nm in a UV-1800 spectrophotometer (Shimadzu, Japan). The content of total flavonoids was calculated as:

$$\text{Content of flavonoids} = \frac{A_{420} \times V}{m \times d}$$

where, A₄₂₀ were the absorbance at 420 nm, V were total volume of the extract, m were the extraction quality from the leaf of each sample (1 g), d were the dilution multiple.

As described by Sharma and Bhat⁵¹, 2 mL of each of the filtrates, as well as two milliliters of ethanol (blank control), were added with 2 ml of 0.04 mmol/L ethanol solution of 1-diphenyl-2-picrylhydrazyl (DPPH), incubated in dark for 20 min, and detected the absorbance at 517 nm in an UV-1800 spectrophotometer. The free radical scavenging activities were calculated as:

$$\text{Free radical scavenging activity} = \frac{1 - (A_i - A_b)}{A_n} \times 100$$

where, A_i, A_b and A_n were the absorbance of the induced samples, the non-inducing samples and the blank control.

Quantification of flavonal constituents and anthocyanidin. Ten microliters of each of the filtrates were loaded into HPLC (Agilent 1260) equipped with Brownlee SPP C18 column (E-Merck, 2.7 μm, 4.6 × 150 nm). Gradient elution was conducted with 80% mobile phase A (98% H₂O and 2% H₃PO₄) and 20% mobile phase B (CH₃Cl) for 5 min, 55% mobile phase A and 45% mobile phase B for 43 min, and 80% mobile phase A and 20% mobile phase B for 2 min at a flow rate of 1 ml/min and column temperature of 30 °C. The flavonal constituents (rutin, quercetin and kaempferol) were monitored at 360 nm and identified by comparison of retention time with their authentic samples. Their relative contents were quantified and expressed as percentage peak area.

As described by Tanaka *et al.*⁵², one leaf of each sample of 0 (control), 1, 2, 3, 4, 5 and 6 d of the induction, was pulverized to fine powder in liquid nitrogen, extracted with acidified (1% HCl) methanol in dark with shaking for 48 h, and centrifuged at 4000 g for 10 min. The supernatant was used to determine for absorbance at 535 nm in an UV-1800 spectrophotometer. The anthocyanidin content was indicated by absorption value.

Determination of MDA content. As described by Yu *et al.*⁵³, the other leaf of the each sample of 0 (control), 1, 2, 3, 4, 5 and 6 d of the induction was pulverized with 10% trichloroacetic acid (TCA) and centrifuged at 4000 g for 10 min. Two milliliters of the supernatant was added with 2 mL of 0.06% thiobarbituric acid (TBA), and bathed in boiling water for 10 min. After cooled, the samples were centrifuged at 7000 g for 5 min. The supernatant was determined for absorbance at 450, 532, and 600 nm, respectively, in an UV-1800 spectrophotometer. The MDA content was calculated as:

$$\text{MDA content} = [6.452 \times (A_{532} - A_{600}) - 0.559 \times A_{450}] \times [V \div (V' \times W)]$$

where, A_{450} , A_{532} , and A_{600} were absorbance at 450, 532, and 600 nm, respectively. V , V' , and W were total volume of the extract, the determined volume (2 mL), and the fresh weight of the sample.

Received: 24 January 2019; Accepted: 22 October 2019;

Published online: 27 December 2019

References

- Lang, K., Chen, X. & Luo, Y. Flora reipublicae popularis sinicae (Flora of China, Volume XVII) Angiospermae 220–227 (Science Press Beijing, 1999).
- Takatsuki, S., Wang, J. D. & Narui, T. Studies on the components of crude drug 'kim-soan-lian'. *J Jap Bot* **67**, 121–123 (1992).
- Cui, S. C. *et al.* Antihyperglycemic and antioxidant activity of water extract from *Anoectochilus roxburghii* in experimental diabetes. *Exp Toxicol Pathol* **65**, 485–488 (2013).
- Hoi, T. M. *et al.* Flavonoids from *Anoectochilus annamensis* and their anti-inflammatory activity. *Nat Prod Commun* **11**, 613–614 (2016).
- Yang, Z. *et al.* Protective effect of *Anoectochilus roxburghii* polysaccharide against CCl_4 -induced oxidative liver damage in mice. *Inter J Biol Macromol* **96**, 442–450 (2017).
- Ye, S., Shao, Q. & Zhang, A. *Anoectochilus roxburghii*: A review of its phytochemistry, pharmacology, and clinical applications. *J Ethnopharmacol* **209**, 184–202 (2017).
- Zhang, Y., Cai, J., Ruan, H., Pi, H. & Wu, J. Antihyperglycemic activity of kinsenoside, a high yielding constituent from *Anoectochilus roxburghii*, in streptozotocin diabetic rats. *J Ethnopharmacol* **114**, 141–145 (2007).
- Du, X. M., Sun, N. Y., Irino, N. & Shoyama, Y. Glycosidic constituents from *in vitro* *Anoectochilus formosanus*. *Chem Pharm Bull* **48**, 1803–1804 (2000).
- Zhang, F., Lv, Y., Dong, H. & Guo, S. Analysis of genetic stability through intersimple sequence repeats molecular markers in micropropagated plantlets of *Anoectochilus formosanus* Hayata, a medicinal plant. *Biol Pharm Bull* **33**, 384–388 (2010).
- Ma, Z., Li, S., Zhang, M., Jiang, S. & Xiao, Y. Light intensity affects growth, photosynthetic capability, and total flavonoid accumulation of *Anoectochilus* plants. *Hortscience* **45**, 863–867 (2010).
- Christie, J. M. & Jenkins, G. I. Distinct UV-B and UV-A/blue light signal transduction pathways induce chalcone synthase gene expression in *Arabidopsis* cells. *Plant Cell* **8**, 1555–1567 (1996).
- Colla, G. *et al.* Effects of saline stress on mineral composition, phenolic acids and flavonoids in leaves of artichoke and cardoon genotypes grown in floating system. *J Sci Food Agri* **93**, 1119–1127 (2013).
- Zhu, H. *et al.* Effects of low light on photosynthetic properties, antioxidant enzyme activity, and anthocyanin accumulation in purple pak-choi (*Brassica campestris* ssp. *Chinensis* Makino). *PLoS One* **12**, e0179305 (2017).
- Afreen, F., Zobayed, S. M. & Kozai, T. Spectral quality and UV-B stress stimulate glycyrrhizin concentration of *Glycyrrhiza uralensis* in hydroponic and pot system. *Plant Physiol Biochem* **43**, 1074–1081 (2005).
- Zhang, X., Abraham, C., Colquhoun, T. A. & Liu, C. J. A proteolytic regulator controlling chalcone synthase stability and flavonoid biosynthesis in *Arabidopsis*. *Plant Cell* **29**, 1157–1174 (2017).
- Winkel-Shirley, B. Flavonoid biosynthesis. a colorful model for genetics, biochemistry, cell biology, and biotechnology. *Plant Physiol* **126**, 485–493 (2001).
- Shih, C. C., Wu, Y. W. & Lin, W. C. Scavenging of reactive oxygen species and inhibition of the oxidation of low density lipoprotein by the aqueous extraction of *Anoectochilus formosanus*. *Am J Chin Med* **31**, 25–36 (2003).
- Sankari, S. L., Babu, N. A., Rani, V., Priyadharsini, C. & Masthan, K. M. Flavonoids-clinical effects and applications in dentistry: A review. *J Pharm Bioallied Sci* **6**, S26–29 (2014).
- Ververidis, F. *et al.* Biotechnology of flavonoids and other phenylpropanoid-derived natural products. Part I: Chemical diversity, impacts on plant biology and human health. *Biotechnol J* **2**, 1214–1234 (2007).
- Ferrer, J. L., Austin, M. B., Stewart, C. J. & Noel, J. P. Structure and function of enzymes involved in the biosynthesis of phenylpropanoids. *Plant Physiol Biochem* **46**, 356–370 (2008).
- Han, Y. Cloning and characterization of a novel chalcone synthase gene from *Phalaenopsis hybrid* Orchid flowers. *Russ J Plant Physiol* **53**, 250–258 (2006).
- Reimold, U., Kroger, M., Kreuzaler, F. & Hahlbrock, K. Coding and 3' non-coding nucleotide sequence of chalcone synthase mRNA and assignment of amino acid sequence of the enzyme. *EMBO J* **2**, 1801–1805 (1983).
- Awasthi, P. *et al.* Cloning and expression analysis of chalcone synthase gene from *Coleus forskohlii*. *J Genet* **95**, 647–657 (2016).
- Bovy, A., Schijlen, E. & Hall, R. D. Metabolic engineering of flavonoids in tomato (*Solanum lycopersicum*): the potential for metabolomics. *Metabolomics* **3**, 399–412 (2007).
- Guo, D. *et al.* Overexpression of *CtCHS1* increases accumulation quinochalcone in safflower. *Front Plant Sci* **8**, 1409–1422 (2017).
- Franken, P. *et al.* The duplicated chalcone synthase genes *C2* and *Whp* (white pollen) of *Zea mays* are independently regulated; evidence for translational control of *Whp* expression by the anthocyanidin intensifying gene *In*. *EMBO J* **10**, 2605–2612 (1991).
- Wani, T. A. *et al.* Molecular and functional characterization of two isoforms of chalcone synthase and their expression analysis in relation to flavonoid constituents in *Grewia asiatica* L. *PLoS One* **12**, e0179155 (2017).
- Edahiro, J. I., Nakamura, M., Seki, M. & Furusaki, S. Enhanced accumulation of anthocyanidin in cultured strawberry cells by repetitive feeding of L-phenylalanine into the medium. *J Biosci Bioeng* **99**, 43–47 (2005).
- Masoumian, M., Arbakariya, A., Syahida, A. & Maziah, M. Effect of precursors on flavonoid production by *Hydrocotyle bonariensis* callus tissues. *Afri J Biotechnol* **10**, 6021–6029 (2011).
- Erkan, M., Wang, S. Y. & Wang, C. Y. Effect of UV treatment on antioxidant capacity, antioxidant enzyme activity and decay in strawberry fruit. *Posth Biol Technol* **48**, 163–171 (2008).

31. Jiang, T., Jahangir, M. M., Jiang, Z., Lu, X. & Ying, T. Influence of UV-C treatment on antioxidant capacity, antioxidant enzyme activity and texture of postharvest shiitake (*Lentinus edodes*) mushrooms during storage. *Posth Biol Technol* **56**, 209–215 (2010).
32. Shen, Y., Jin, L., Xiao, P., Lu, Y. & Bao, J. Total phenolics, flavonoids, antioxidant capacity in rice grain and their relations to grain color, size and weight. *J Cereal Sci* **49**, 106–111 (2009).
33. Tegelberg, R. & Julkunen-Tiitto, R. Quantitative changes in secondary metabolites of dark-leaved willow (*Salix myrsinifolia*) exposed to enhanced ultraviolet-B radiation. *Physiol Plant* **113**, 541–547 (2010).
34. Abrol, E., Vyas, D. & Koul, S. Metabolic shift from secondary metabolite production to induction of anti-oxidative enzymes during NaCl stress in *Swertia chirata*, Buch.-Ham. *Acta Physiol Plant* **34**, 541–546 (2012).
35. Gengmao, Z., Shihui, L., Xing, S., Yizhou, W. & Zipan, C. The role of silicon in physiology of the medicinal plant (*Lonicera japonica* L.) under salt stress. *Sci Rep* **5**, 12696 (2015).
36. Hrazdina, G., Zobel, A. M. & Hoch, H. C. Biochemical, immunological, and immunocytochemical evidence for the association of chalcone synthase with endoplasmic reticulum membranes. *Proc Natl Acad Sci USA* **84**, 8966–8970 (1987).
37. Wang, C. *et al.* Isolation and characterization of a novel chalcone synthase gene family from mulberry. *Plant Physiol Biochem* **115**, 107–118 (2017).
38. Buer, C. S. & Muday, G. K. The *transparent testa4* mutation prevents flavonoid synthesis and alters auxin transport and the response of *Arabidopsis* roots to gravity and light. *Plant Cell* **16**, 1191–1205 (2004).
39. Feucht, W., Treutter, D. & Polster, J. Flavanol binding of nuclei from tree species. *Plant Cell Rep* **22**, 430–436 (2004).
40. Peer, W. A. *et al.* Flavonoid accumulation patterns of transparent testa mutants of *Arabidopsis*. *Plant Physiol* **126**, 536–548 (2001).
41. Saslowsky, D. E., Warek, U. & Winkel, B. S. Nuclear localization of flavonoid enzymes in *Arabidopsis*. *J Biol Chem* **280**, 23735–23740 (2005).
42. Faktor, O., Kooter, J. M., Dixon, R. A. & Lamb, C. J. Functional dissection of a bean chalcone synthase gene promoter in transgenic tobacco plants reveals sequence motifs essential for floral expression. *Plant Mol Biol* **32**, 849–859 (1996).
43. Hartmann, U. *et al.* Identification of UV/blue light-response elements in the *Arabidopsis thaliana* chalcone synthase promoter using a homologous protoplast transient expression system. *Plant Mol Biol* **36**, 741–754 (1998).
44. Qian, W. *et al.* Identification of a bHLH-type G-box binding factor and its regulation activity with G-box and Box I elements of the *PsCHS1* promoter. *Plant Cell Rep* **26**, 85–93 (2007).
45. Yu, H. *et al.* Cloning and characterization of BES1/BZR1 transcription factor genes in maize. *Plant Growth Regul* **86**, 235–249 (2018).
46. Lin, Y. J. & Zhang, Q. Optimizing the tissue culture conditions for high efficiency transformation of indica rice. *Plant Cell Rep* **23**, 540–547 (2005).
47. Zhang, G. *et al.* Characterization of reference genes for quantitative real-time PCR analysis in various tissues of *Anoectochilus roxburghii*. *Mol Biol Rep* **39**, 5905–5912 (2012).
48. Livak, K. J. & Schmittgen, T. D. Analysis of relative gene expression data using real-time quantitative PCR and the $2^{-\Delta\Delta CT}$ method. *Methods* **25**, 402–408 (2001).
49. Liu, Y. G., Mitsukawa, N., Oosumi, T. & Whittier, R. F. Efficient isolation and mapping of *Arabidopsis thaliana* T-DNA insert junctions by thermal asymmetric interlaced PCR. *Plant J* **8**, 457–463 (1995).
50. Chen, L. *et al.* Continuous determination of total flavonoids in platycladus orientalis (L.) franco by dynamic microwave-assisted extraction coupled with on-line derivatization and ultraviolet-visible detection. *Anal Chim Acta* **596**, 164–170 (2007).
51. Sharma, O. P. & Bhat, T. K. DPPH antioxidant assay revisited. *Food Chem* **113**, 1202–1205 (2009).
52. Tanaka, A. *et al.* A new *Arabidopsis* mutant induced by ion beams affects flavonoid synthesis with spotted pigmentation in testa. *Genes Genet Syst* **72**, 141–148 (1997).
53. Yu, H. *et al.* Cloning and characterization of vacuolar H⁺-pyrophosphatase gene (*AnVP1*) from *Ammopiptanthus nanus*, and its heterologous expression enhances osmotic tolerance in yeast and *Arabidopsis thaliana*. *Plant Growth Regul* **81**, 1–13 (2017).

Acknowledgements

This work was supported by Education Scientific Fund for Young Teachers from Fujian Education Department [JA15470] and Medicinal Plants Development and Utilization Center of Fujian [ZD1601].

Author contributions

L.Y. carried out the experiments, interpreted the results and wrote the manuscript. J.C.Z., J.T.Q. and G.H. took part in some of the experiments. H.Q.Y. provided technical support. W.C.L. and F.L.F. conceived and designed the research. All the authors read and approved the final manuscript.

Competing interests

The authors declare no competing interests.

Additional information

Supplementary information is available for this paper at <https://doi.org/10.1038/s41598-019-56821-0>.

Correspondence and requests for materials should be addressed to W.C.L. or F.L.F.

Reprints and permissions information is available at www.nature.com/reprints.

Publisher's note Springer Nature remains neutral with regard to jurisdictional claims in published maps and institutional affiliations.



Open Access This article is licensed under a Creative Commons Attribution 4.0 International License, which permits use, sharing, adaptation, distribution and reproduction in any medium or format, as long as you give appropriate credit to the original author(s) and the source, provide a link to the Creative Commons license, and indicate if changes were made. The images or other third party material in this article are included in the article's Creative Commons license, unless indicated otherwise in a credit line to the material. If material is not included in the article's Creative Commons license and your intended use is not permitted by statutory regulation or exceeds the permitted use, you will need to obtain permission directly from the copyright holder. To view a copy of this license, visit <http://creativecommons.org/licenses/by/4.0/>.

© The Author(s) 2019